Ionic Permeation and Blockade in Ca^{2+}-activated K^+ Channels of Bovine Chromaffin Cells

GARY YELLEN

From the Section of Molecular Neurobiology and the Department of Physiology, Yale University School of Medicine, New Haven, Connecticut 06510

ABSTRACT Single channel currents through Ca^{2+}-activated K^+ channels of bovine chromaffin cells were measured to determine the effects of small ions on permeation through the channel. The channel selects strongly for K^+ over Na^+ and Cs^+, and Rb^+ carries a smaller current through the channel than K^+. Tetraethylammonium ion (TEA^+) blocks channel currents when applied to either side of the membrane; it is effective at lower concentrations when applied externally. Millimolar concentrations of internal Na^+ reduce the average current through the channel and produce large fluctuations (flicker) in the open channel currents. This flickery block is analyzed by a new method, amplitude distribution analysis, which can measure block and unblock rates in the microsecond time range even though individual blocking events are not time-resolved by the recording system. The analysis shows that the rate of block by Na^+ is very voltage dependent, but the unblock rate is voltage independent. These results can be explained easily by supposing that current flow through the channel is diffusion limited, a hypothesis consistent with the large magnitude of the single channel current.

INTRODUCTION

In the process of permeation through a selective ion channel, ions must interact with one or more specific chemical sites that distinguish between the various ionic species, allowing some, but not others, to pass. Some of the important sites for ion interaction are those where ions may bind stably (energy wells), while other ion-selective sites may be points of maximum resistance to ion passage (energy barriers). These chemical sites can be studied by the same approach used for other specific sites on proteins: analogues of the natural ligand may be used as probes to determine the specifics of ligand interaction with the sites. This approach has been productively applied to many ion channels to measure the physical and chemical specificity of their permeability pathways (reviewed by Hille, 1975; Latorre and Miller, 1983), in an effort to understand the mechanism

Address reprint requests to Dr. Gary Yellen, Graduate Dept. of Biochemistry, Brandeis University, Waltham, MA 02254.

J. GEN. PHYSIOL. © The Rockefeller University Press · 0022-1295/84/08/0157/30 $1.00

Volume 84 August 1984 157–186

that allows up to 10^8 ions per second to cross the membrane while distinguishing miniscule differences (0.4 Å) in ionic radius. I have used this approach to study permeation in the large-conductance, Ca^{2+}-activated K^+ channels of bovine chromaffin cells. Some small ions pass through this Ca^{2+}-activated K^+ channel, and others block the current normally carried by K ions.

Channel blockers constitute a class of molecules that reduce the current through ion channels by a common mechanism: they completely obstruct channel current for some short period of time. Various channel blockers produce different changes in the appearance of single channel records, an observation that may be explained by supposing that individual blockers obstruct channel currents for different lengths of time, relative to the bandwidth of the recording system. Three classes of blockers of the Ca^{2+}-activated K^+ channel can be distinguished on this basis. Slow blockers, such as nonyltriethylammonium ion (C_9) and Ba ion, produce clearly resolved interruptions in single channel currents; each block event looks like a closing of the channel. Fast blockers, such as internally applied Cs ion, produce frequent, extremely brief interruptions of the channel current that can only be detected as an apparent reduction in the level of open channel current. An intermediate class of blockers, including internally applied Na^+, produces rapid fluctuations in current during a channel opening, because of interruptions long enough to detect but too brief to resolve as individual events. Such fluctuations may be called "flicker," and the blockers that produce them, "flickery blockers."

Information about the rates of block and unblock for different blockers under different conditions can tell us about the chemical nature of the channel and its interaction with ions. Each class of blocker must be studied with a different kind of measurement. Fast blockers are studied by measuring the fractional reduction in the apparent open channel current. Slow blockers can be studied simply by measuring the frequency and duration of the interruptions in channel current. Flickery blockers can be studied by the new method, described here, of amplitude distribution analysis. This analysis extracts the block and unblock rates from the shape of the distribution of current amplitudes during channel flicker.

MATERIALS AND METHODS

Experimental Methods

Ca^{2+}-activated K^+ channels from bovine adrenal medullary chromaffin cell membranes were studied in detached inside-out or outside-out membrane patches as described by Horn and Patlak (1980) and Hamill et al. (1981). The cultured chromaffin cells were a generous gift of T. Hoshi and Dr. J. Rothlein (Yale University School of Medicine), and were prepared by the method of Kilpatrick et al. (1980) as modified by Wilson and Viveros (1981). Patch pipettes were prepared as described in Hamill et al. (1981), using Boralex borosilicate micropipettes (100 μl; Rochester Scientific, Rochester, NY) coated with Sylgard (Dow Corning, Midland, MI) and heat-polished to ~0.5 μm i.d. They typically had a resistance of 4 MΩ when filled with any of the isotonic salines used. All of the salines used were filtered immediately before use with a 0.2-μm membrane filter (Acrodisc; Gelman Sciences, Ann Arbor, MI) to remove small particles, which might interfere with the sealing of pipettes to the cells. A bare, chloridized Ag wire was used as the electrode

within the patch pipette, and a similar wire within an agar/saline bridge was used as the bath ground. The patch clamp amplifier used essentially the same circuit as that described by Hamill et al. (1981), with the addition of a sample-and-hold amplifier for automatically adjusting a junction potential correction to give zero current. The junction correction was adjusted immediately before sealing onto a cell. It was routinely checked after recording from a patch, when the patch had broken; it was usually <1 mV and never >5 mV different from the true zero-current potential, measured with the pipette tip in the bath solution used for recording. This suggests that neither drift in the circuitry nor liquid junction potential differences are a serious problem in these experiments. Significant electrode polarization was not expected because of the small size of the currents.

All experiments were performed at room temperature (21–25°C). Experimental values are reported as mean ± SEM, except where indicated.

PERFUSION Solutions were delivered to the exposed face of the detached membrane patch by a variation of the multiple-barrel perfusion system described earlier (Yellen, 1982). The patch pipette with a membrane patch at the tip was moved into the mouth of a perfusion pipette containing the desired solution, and the solution was allowed to flow continuously during the recording. Flow through the perfusion pipettes was turned on or off by a screw clamp attached to the supply tubing; only the solution currently in use was allowed to flow.

SOLUTIONS Saline solutions were always prepared with a mixture of the chloride and hydroxide forms of the alkali metal of interest, and their pH was adjusted with HCl so as to have precisely the nominal concentration of the alkali metal ion and no significant content of other alkali metals. All external solutions (used in the pipette for inside-out patches, and in the perfusion system for outside-out patches) contained 2 mM $CaCl_2$, 1 mM $MgCl_2$, and 10 mM HEPES at pH 7.2, in addition to 160 mM of the alkali metal cation with Cl^- as the counterion. All of the permeation information presented here is from analysis during a time when just a single channel was open. Typically, patches from chromaffin cells contained 3–10 of these large Ca^{2+}-activated K^+ channels (as judged roughly from the highest overlap level seen during large depolarizations). The internal solutions always contained a Ca^{2+}/EGTA buffer to set the free Ca^{2+} at a level high enough to activate channels at depolarized potentials, but low enough to prevent too many overlapping openings. The free Ca^{2+} used was nominally either 0.3 or 1 μM, as computed from the binding constants given in Martell and Smith (1974) and corrected for H ion activity. The standard internal solution with 0.3 μM free Ca^{2+} contained (in mM): 160 KCl/KOH, 10 HEPES, 1 $MgCl_2$, 5 EGTA, and 3.8 $CaCl_2$ at pH 7.2. The 1-μM free Ca^{2+} solution had 5 EGTA and 4.57 $CaCl_2$. When TEA^+ or Cs^+ was used in the internal solution, a sufficient amount of 1-M stock solution was added to the standard internal solution to make the desired concentration.

DATA ACQUISITION AND STIMULATION Membrane current was filtered with an eight-pole tunable low-pass Bessel filter (model 902LPF; Frequency Devices, Haverhill, MA) and sampled into a PDP 11/23 computer (Digital Equipment Corp., Maynard, MA) at intervals of between 10 and 400 μs using a 12-bit analog-to-digital converter (DT2782A; Data Translation, Marlboro, MA). The usual sampling rate was one point per 100 μs; the usual filter setting was 4 kHz. Voltage stimuli were delivered to the clamp command input by a 12-bit D/A converter controlled by the computer and run synchronously with sampling.

USE OF RAMP STIMULI TO DETERMINE OPEN CHANNEL I-V RELATIONSHIP A rapid ramp voltage clamp stimulus was used to measure quickly the open channel current-voltage relationship for single channels (Yellen, 1982). The current measured during a ramp stimulus corresponds to the leakage characteristics of the seal when no channels are

open, and to the leakage plus the open channel current when one channel is open. If a ramp stimulus is applied repeatedly to a patch of membrane with an active channel, channel openings occur at random during the ramp (for an example, see Yellen, 1982). To construct a complete *I-V* relationship, segments of each record that contained zero or one channel open were manually identified to the computer, which averaged them point by point. The open channel *I-V* was obtained by subtracting the average leakage *I-V* (with zero channels open) from the average *I-V* with one channel open.

There are three sources of artifacts in determining channel *I-V* curves from ramp data. The first is channel flicker: if there are many unresolved closings during a long channel opening, the apparent open channel current measured from ramps may be smaller than the apparent current obtained by visually drawing a line through the top of the channel currents in steady state records. All of the data presented here have little problem in this respect; channel currents observed at steady state correlate quite well with those measured by ramps. However, it is important to avoid including brief closings in the open channel segments chosen for averaging. The second source of artifact is capacitive current; this can be eliminated by electronic compensation. In any case, the open channel *I-V*'s were measured as the difference between two experimental *I-V* curves with exactly the same capacitive artifacts. The third and most serious source of artifact is heterogeneity among individual channels of the same general type. Individual Ca^{2+}-activated K^+ channels, as reported elsewhere (Methfessel and Boheim, 1982), may vary by ~20% in their conductance. The cumulative average of open channel ramp records was displayed while selecting ramp segments to include in the average, and traces that showed significantly different open channel currents from those in the cumulative average were not included in the average. The *I-V* curves shown here and their relationship to each other are consistent in experiments done on at least four different patches, with several hundred individual ramp traces under each ionic condition for each patch.

To collect ramp data for these voltage-dependent, Ca^{2+}-activated K^+ channels, the likelihood of seeing channel openings at less depolarized voltages was increased by stepping to a depolarized voltage to activate the channels, and then applying a rapid, descending ramp stimulus. Results obtained from ascending and descending ramps are exactly comparable.

MEASUREMENT OF WELL-RESOLVED OPEN AND CLOSED DURATIONS Records of channel openings interrupted by C_9 blocking events were analyzed by marking a threshold at 50% of the open channel level and considering each sample point above the threshold to be open and each point below to be closed. The virtues of the 50% threshold are discussed by Colquhoun and Sigworth (1983).

Analysis of Channel Flicker from Amplitude Distributions

Channel flicker can be analyzed by assuming that it is composed of filtered (unresolved) transitions between two discrete levels. The analysis consists in comparing the measured amplitude distribution of the flicker with a theoretical amplitude distribution that depends on the filter cut-off frequency and the transition rates between the two states, and finding the transition rates that produce the best fit between theory and experiment. The theory makes two assumptions: (*a*) that the flicker is composed of filtered fluctuations between two states of known conductance, and (*b*) that the transition process is described by a two-state Poisson process.

This section treats the theory that describes the amplitude distribution for a filtered, two-state process. The theory for a two-state process and a first-order filter can be solved exactly; it has been treated in detail by FitzHugh (1983), and is briefly described in the Appendix. For a simple two-state (open and blocked) Poisson process filtered through a

single time constant filter, the shape of the amplitude histogram of the filtered process bears a simple relationship to the unblocking and blocking rates α and β and the filter time constant τ.

The open state is the unblocked state of the channel; it is assumed to pass a current equal to one (dimensionless); the blocked state is assumed to pass zero current.

AMPLITUDE DISTRIBUTION WITH A FIRST-ORDER FILTER The differential equations governing the simple case of a two-state blocking-unblocking process and a first-order filter are derived in the Appendix. They describe the amplitude distribution of a two-state process with rates α and β after filtering with a first-order filter of time constant τ. The steady state solution to these equations gives the amplitude distribution of the filter output (y), which is a beta distribution described by the following probability density function, $f(y)$:

$$f(y) = y^{a-1}\,(1 - y)^{b-1}/B(a, b), \tag{1}$$

where

$$a = \alpha\tau, \qquad b = \beta\tau, \tag{2a, b}$$

and

$$B(a, b) = \int_0^1 y^{a-1}\,(1 - y)^{b-1}\,dy \qquad \text{(beta function)}. \tag{3}$$

On the range of amplitudes (y) from 0 to 1, the probability of finding a filter output amplitude in the interval (y, $y + dy$), where dy is very small, is equal to $f(y)\,dy$.

AMPLITUDE DISTRIBUTION WITH A MULTISTAGE FILTER The form of the amplitude distribution for a process filtered with a multistage (higher-order) filter cannot be solved using the same mathematical approach, since the trajectory of the filtered process depends not only upon the state of the original process (open or blocked) and on the value of the filter output (y), but also on the value of the time derivatives of y. The filtered process is no longer a simple function of a two-state Markov process, but is now a multivariate, continuous state space process, for which it is difficult to find an analytical solution. It is impractical to use a single time constant filter for single channel recording experiments, because the attenuation of noise at high frequencies is very poor (e.g., for a 1-kHz single-pole filter, noise at 10 kHz is only attenuated by a factor of 10). However, I have measured the amplitude distribution for a simulated two-state process filtered by the eight-pole Bessel filter used for experiments, over a large range of opening and blocking rates. For fast processes, the amplitude histograms from the simulation can be described excellently by beta distributions, and the parameters of the beta distribution can be predicted by positing an equivalent single-pole filter corresponding to a particular setting of the tunable Bessel filter. The empirical formula relating the 3-dB attenuation frequency of the Bessel filter (f) to the equivalent single-pole filter frequency (f_0) is

$$f_0 = 0.7f, \tag{4a}$$

and the effective time constant (τ) is

$$\tau = 0.228/f. \tag{4b}$$

This value is 57 μs for the usual filter setting for these experiments of 4 kHz. The correspondence to the theory for the single-pole filter is good for $a, b > 2$; for processes slower than this, the density near the ends of the interval [0, 1] deviates from the theory.

These slower processes may be studied by refiltering the data using a lower filter setting (see below).

SHAPE OF THE AMPLITUDE DISTRIBUTION For a very slow process, all of the density of the amplitude distribution is near zero and one, because the filtered process still has well-resolved openings and closings (Fig. 1*A*). For a very fast process, the amplitude

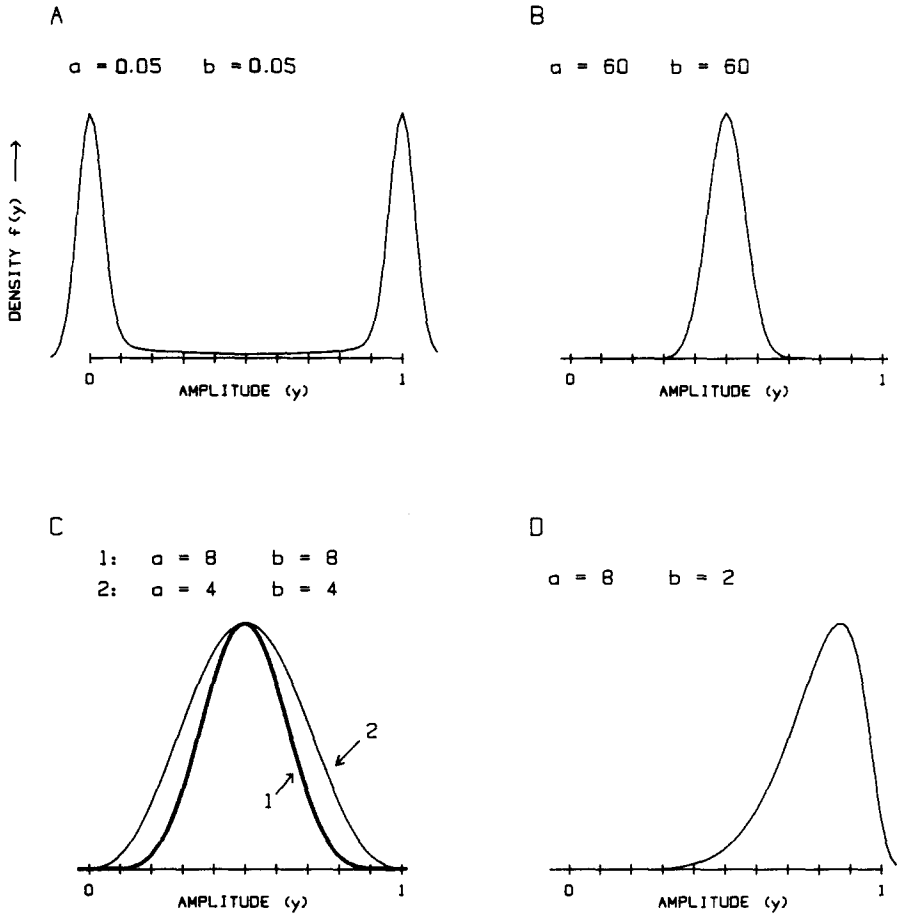

$$\text{BLOCKED} \underset{\beta}{\overset{\alpha}{\rightleftharpoons}} \text{OPEN}$$

τ = FILTER TIME CONSTANT

$a = \alpha\tau \qquad b = \beta\tau$

distribution is a single sharp peak (Fig. 1*B*) corresponding to the time-averaged value determined by the blocking and unblocking rates (Coronado and Miller, 1979). For a fast process that does not correspond to this limiting case, the distribution has a single peak which is narrow and Gaussian, and which becomes broader as the process gets slower (Fig. 1*C*). Broader distributions are not exactly Gaussian in shape. Unequal blocking and unblocking rates give a skewed distribution (Fig. 1*D*). The shape of the amplitude distribution is quite sensitive to changes in the blocking and unblocking rates over a range for a and b from ~2 to 20.

There is a range of processes that are too slow to be measured critically by this method but too fast to be resolved as individual openings and closings. These processes can be studied by refiltering the data with a slower filter before compiling the amplitude histograms, which effectively raises a and b into this range by raising τ. This was accomplished by converting the digitized data back into an analog signal, filtering the analog signal with the same eight-pole Bessel filter used for experiments, and redigitizing the filtered signal.

COLLECTION AND PROCESSING OF AMPLITUDE HISTOGRAMS Sections of single channel records that contained one active channel, usually including small sections of baseline (no channels open), were selected for inclusion in amplitude histograms. Individual amplitude histograms contained contributions from an average of 200 ms of open channel flicker; at least two to three histograms were compiled for each experimental condition for each experiment that was used in the analysis. The usual amplitude bin size for histogram collection was 0.8 pA. A Gaussian curve was fitted to the peak corresponding to the baseline; the average standard deviation was 1.1 bin for records collected at 4 kHz. The Gaussian curve was then subtracted from the histogram to remove the closed channel contribution to the histogram; this procedure did not significantly change any of the fits to the histograms, since histogram analysis was not attempted when the baseline significantly overlapped the open channel level.

FITTING OF A BETA DISTRIBUTION TO THE MEASURED AMPLITUDE HISTOGRAMS A computer-generated beta distribution was fitted by eye to each amplitude histogram by adjusting the two parameters, a and b, of the theoretical distribution. In order to compensate for the broadening of the experimental distribution by unrelated noise, the theoretical distribution was also broadened by convolving it with the Gaussian curve used to fit the amplitude distribution of the baseline (closed channel) noise. Fits were almost always quite good (but see below). The unblocking and blocking rates α and β were then computed from the measured a and b of the redistribution using the definitions of a and b in Eqs. 2a and b and the empirical filter time constant from Eq. 4.

Before fitting a beta distribution, it was necessary to know the open channel current through the unblocked channel in order to normalize the amplitudes of the experimental

FIGURE 1. (*opposite*) Theoretical behavior of amplitude distributions. These computed amplitude distributions are computed beta distributions (see Eq. 1 and Appendix) with the peak density normalized to be constant. The probability density on the ordinate is plotted against amplitude on the abscissa. The abscissa ranges from 0 to 1 (divided into tenths); 0 corresponds to the closed channel current amplitude and 1 to the open channel. Each theoretical distribution is convolved with a Gaussian with a half-width equal to 5% of the open channel amplitude; this accounts for the effect of experimental noise on the measured amplitude distributions, and is similar to the procedure employed in fitting experimental amplitude distributions. The values a and b are relative rate constants, defined at the bottom of the figure and in the text. See text for further details.

distribution. The variation in the conductance of the channel from experiment to experiment made it advisable to determine the open channel current amplitude for each experiment. This was easily done with experiments on inside-out patches by switching to an internal solution with no Na^+. For experiments with outside-out patches, however, it was necessary to extrapolate the open channel current from the peak amplitude of the currents when the block was relieved by moderate amounts (~20 mM) of external K^+ (see Yellen, 1984*b*). This extrapolated channel size was used to analyze all of the histograms from a single experiment. Varying the size used in the analysis by ±20% did change the absolute values measured for α and β, and usually made the fits worse than with the extrapolated value, but never changed the qualitative results concerning changes in α and β. Rates measured from different patches agreed quite well, but critical comparisons to ascertain the effects of changes in ion concentrations were always done between measurements on the same patch.

There are two potential artifacts that probably account for the occasional experiment that fails to give amplitude distributions that are well fitted by beta distributions (in the range of rates that would be expected to give good fits despite the Bessel filter). The first of these is baseline drift, which can smear out the histogram because the contribution from one record will fail to align properly with the next. This could usually be corrected by automatically finding and subtracting the closed channel baseline for each record before including it in the histogram. The second artifact is produced by inhomogeneity in the open channel current among different Ca^{2+}-activated K^+ channels in the same patch. Including channel flicker from several channels of different sizes in the same histogram will tend to smear out the histogram, causing an underestimate of the block and unblock rates, and sometimes making the histogram too different from a beta distribution to give a reasonable fit. Care was taken to avoid including channel events of different mean amplitudes in the same histogram; it was necessary to include only long bursts, as bursts of only a few milliseconds would show a naturally large fluctuation about the mean.

It is possible to obtain a reasonably smooth amplitude histogram from just a single burst (see the single-burst amplitude histograms in Fig. 8). Such amplitude histograms are free from both types of artifact discussed here. In several experiments, these amplitude histograms were compared with those compiled from many bursts and found to agree well.

RESULTS

Channel Conductance and Selectivity

The Ca^{2+}-activated K^+ channel in chromaffin cell membranes (described by Marty, 1981) has a slope conductance at 0 mV of 265 ± 20 pS (mean ± SD, n = 8) in symmetrical 160 mM KCl solutions at 20–22°C, with a range of observed conductances between 190 and 330 pS. This variability in the channel conductance of Ca^{2+}-activated K^+ channels has been noted by other workers (Methfessel and Boheim, 1982). The relative permeation properties of different cations seem to be quite comparable in individual Ca^{2+}-activated K^+ channels of different sizes seen in this preparation, and the variation in the blocking kinetics described below seems to be uncorrelated with and smaller than the variation in size.

The current-voltage (*I-V*) relationship measured by ramps in symmetrical K^+ is nearly linear (ohmic) over a range from −60 to +70 mV; outside of this range,

the conductance of the channel decreases with increasing voltage (Fig. 2*A*); thus, the *I-V* is said to be sublinear, since the slope falls below that of a straight line at extreme voltages. This sublinearity is not an artifact of the ramp method; the same *I-V* can be measured from the open channel current measured in steady state records at different voltages. A rapid voltage-dependent block, perhaps by

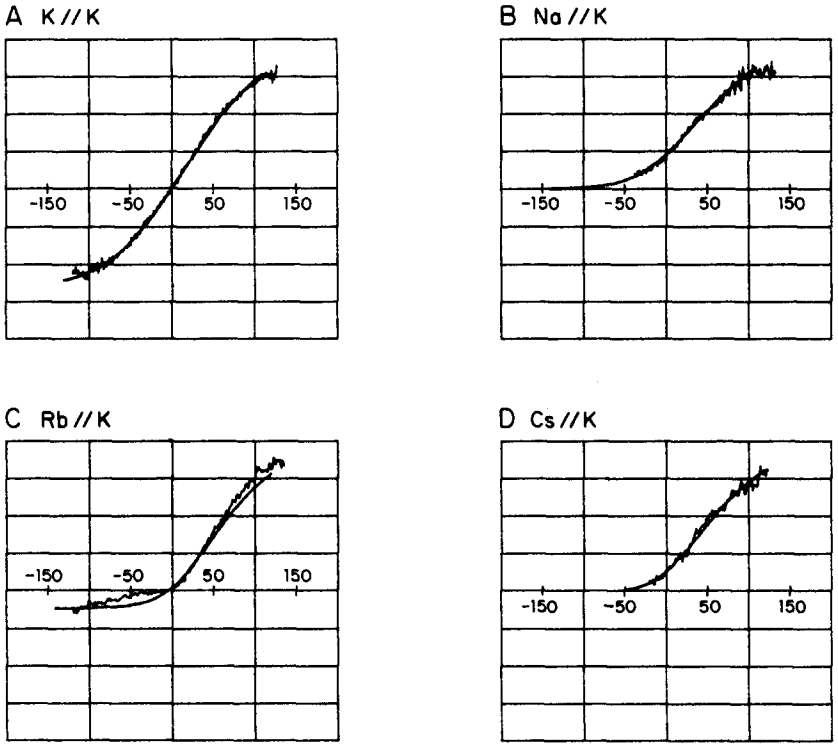

FIGURE 2. Open channel *I-V* relationships with different external cations. The *I-V* curves were measured from ramps under biionic conditions, with a 160-mM concentration of test cation (as labeled) outside and 160 mM K^+ inside (other components of the solutions are described in Materials and Methods). Vertical scale: one box equals 8 pA. The smooth lines are fits to the *I-V*'s generated from the model described below and in Fig. 11. The model has two ion binding sites, repulsion between ions in the channel, and diffusion limitation of ion flow. The sublinearity of the $K^+//K^+$ *I-V* is produced in the model by the diffusion limitation on ion flow. In the model, Na^+ is considered to be inert with respect to the channel when applied to the outside, Rb^+ binds more tightly to K^+ to one of the sites in the channel, and Cs^+ can reach both sites from the outside of the membrane, but cannot pass the innermost barrier to reach the inside solution.

H ions (cf. Cook et al., 1983), might produce this sublinearity. It could also be produced by the intrinsic permeability properties of the channel, or by the phenomenon of diffusion-limited ion flow (see below).

The channel is strongly cation selective, as indicated by the reversal potential for channel currents in the presence of transmembrane salt gradients. When the

outside solution contains 32 mM KCl (plus sucrose to balance the osmotic strength) and the internal solution contains 160 mM KCl, the channel currents reverse at -39 ± 1 mV ($n = 2$). The Nernst potential for K^+ under these conditions is -40 mV; the Nernst potential for Cl^- is $+40$ mV. A perfectly cation-selective channel would be expected to reverse at -40 mV.

This K^+ channel also selects very strongly for K^+ over Na^+, as indicated by the current-voltage relationship with NaCl outside and KCl inside (Fig. 2*B*). As the membrane potential is made more negative, the outward K^+ current becomes smaller, but no inward current (which would necessarily be carried by Na^+, since the channel is cation selective) is detected over the range of potentials studied ($+160$ to -120 mV). Indeed, even at -70 mV, there is an outward current flow through the channel of nearly 1 pA. It appears that the reversal potential, if current does reverse, is more negative than -80 mV; this corresponds to an upper limit for the Na^+/K^+ permeability ratio (as defined by the reversal potential) of ~0.03.

Rb ions can carry inward current through this K^+ channel, as through a variety of other K^+ channels (Chandler and Meves, 1965; Hagiwara and Takahashi, 1974; Hille, 1973; Coronado et al., 1980; Reuter and Stevens, 1980; Gorman et al., 1982). The permeability of Rb^+ through the chromaffin cell Ca^{2+}-activated K^+ channel is nearly the same as that of K^+, as determined from the biionic reversal potential with RbCl outside and KCl inside ($V_{rev} = -4.8 \pm 1.1$ mV, $n = 3$). However, the conductance of the channel at negative potentials, where the current is carried by Rb^+, is much smaller than the conductance when the current is carried by K^+ (cf. Fig. 2, *C* and *A*). This result suggests that Rb^+ decreases its own current by binding to a saturable site in the channel (Hille, 1972; Adams et al., 1981). Rb binding might also be expected to reduce the outward K^+ current below that seen in symmetrical K^+; the failure of Rb^+ to do so and the sharp corner near the reversal potential in the *I-V* with Rb^+ outside indicate that the block by Rb^+ must be very voltage dependent.

Cs^+ Blocks Channel Currents from Either Side of the Membrane

Like external Na^+, external Cs^+ carries no detectable inward current even at very large negative potentials (Fig. 2*D*). However, the outward currents measured at negative potentials with Cs^+ outside are smaller than those measured with Na^+ outside, which indicates that Cs^+ blocks outward current flow throughout the channel in a voltage-dependent fashion (cf. Chandler and Meves [1965] and Adelman and French [1978] on squid axon, and Dubois and Bergman [1977] on node of Ranvier).

Internal Cs ions also block Ca^{2+}-activated K^+ channel currents (Fig. 3), as they do delayed rectifier currents (Chandler and Meves, 1965; Adelman and Senft, 1966; Bezanilla and Armstrong, 1972) and the sarcoplasmic reticulum K^+ channel (Coronado and Miller, 1979). The apparent open channel current is reduced (Fig. 3*A*), and the reduction is more pronounced at depolarized voltages, which should drive internal Cs ions into the channel (Fig. 3*B*).

We can measure the voltage dependence of Cs^+ block in the following way. Blockade of Cs^+ is much too fast for us to observe the discrete open and blocked

states of the channel. Rather, we see the time-averaged value of the current through the channel (Woodhull, 1973; Coronado and Miller, 1979; Horn et al., 1983). The equilibrium between the open and blocked states depends on voltage; in a simple model for blockade, the voltage dependence arises because the blocking ion binds to a site inside the channel, within the transmembrane electric field. This model predicts that the equilibrium between the blocked and open (unblocked) state will be

$$\text{blocked/unblocked} = [\text{B}]/K(0)\exp(F\delta V/RT), \quad (5)$$

where [B] is the blocker concentration, $K(0)$ is the zero-voltage equilibrium constant, and δ is the fraction of the voltage felt at the blocking site (equivalent to the "effective valence" for monovalent ions; Woodhull, 1973). Assuming that the blocked state of the channel carries no current, the time-averaged channel current will be

$$\langle \text{i}(V) \rangle = i_0(V)\,[1 + [\text{B}]/K(0)\exp(F\delta V/RT)]^{-1}, \quad (6)$$

where $i_0(V)$ is the current through the unblocked channel (Coronado and Miller, 1979). For block by internal Cs^+, i_0 is the current in the absence of internal Cs^+; for block by internal Cs^+, it seems reasonable to take the current measured with Na^+ outside as i_0, since the shallow slope of the *I-V* in Na^+ indicates that if external Na^+ blocks at all, the block is not very voltage dependent. The value of δ measured by this method for block by external Cs^+ is quite high (1 ± 0.2, $n = 3$; Fig. 3*C*); this corresponds to a change in affinity of e-fold per 25 mV. Blockade by internal Cs^+ has a low affinity (two experiments with 10 mM internal Cs^+ suggest a K_d of ~100 mM); the δ for block by internal Cs^+ is 0.25 ± 0.1 ($n = 2$; see Fig. 3*C*).

External and Internal TEA^+ Block at Different Sites

Tetraethylammonium ion (TEA^+) has been used pharmacologically to block the currents through K^+ channels in many preparations and to probe the channel's structure (Tasaki and Hagiwara, 1957; Armstrong and Binstock, 1965; Armstrong, 1966; Hille, 1967; Armstrong and Hille, 1972; Thompson, 1977; Hermann and Gorman, 1981; Wong et al., 1982). TEA^+ is an effective blocker of the chromaffin cell Ca^{2+}-activated K^+ channel when applied from either side of the membrane. Internal TEA^+ block appears as a reduction in open channel current (Fig. 4*A*); the block and unblock events must be much too fast to detect. External TEA^+ is effective at lower concentrations than internal TEA^+, and its block is a slower process: it can be detected as a rapid flicker in the channel currents (Fig. 4*B*). One experiment for each condition was analyzed quantitatively.

Internal TEA^+ produces the reduction in the open channel *I-V* shown in Fig. 5*A*. At zero voltage, 10 mM internal TEA^+ reduces the current by 26%; this corresponds to a K_d of 27 mM, which agrees well with Vergara's (1983) value of 35 ± 7 mM for the Ca^{2+}-activated K^+ channel in skeletal muscle T-tubule membranes. The voltage dependence of the block is very small ($\delta = 0.1$, measured as described above for Cs^+; Fig. 5*B*).

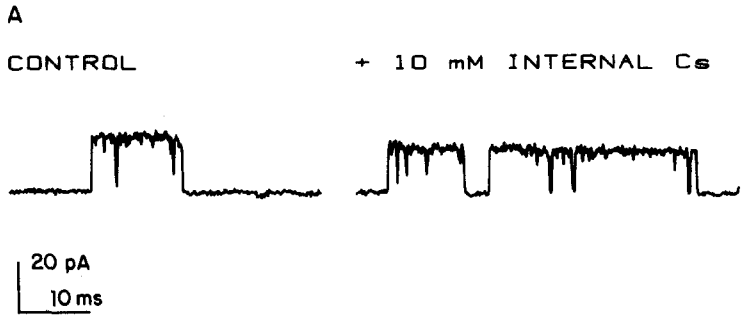
A
CONTROL
+ 10 mM INTERNAL Cs
20 pA
10 ms

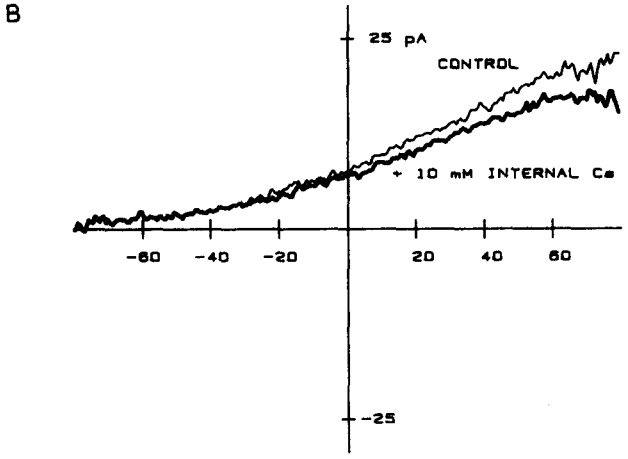
B
25 pA
CONTROL
+ 10 mM INTERNAL Cs
-60
-40
-20
20
40
60
-25

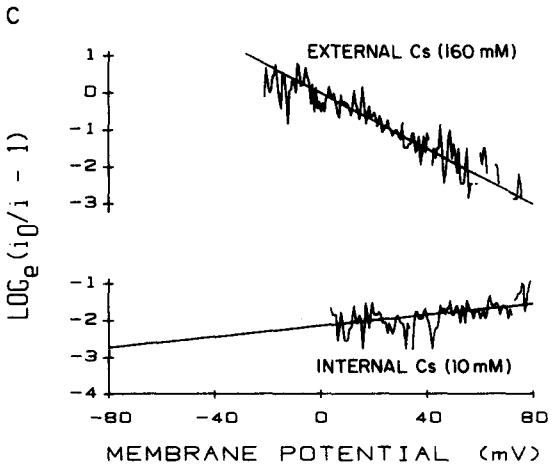
C
EXTERNAL Cs (160 mM)
INTERNAL Cs (10 mM)
LOG$_e$ (i_0/i - 1)
1
0
-1
-2
-3
-4
-80
-40
0
40
80
MEMBRANE POTENTIAL (mV)

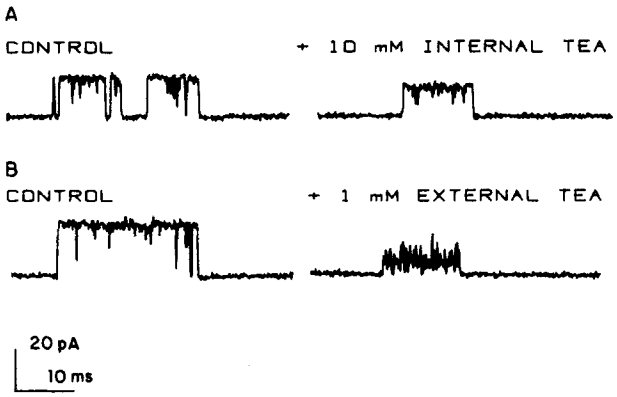

FIGURE 4. Block by internal and external TEA^+ is different. (*A*) Single channel currents in control solution (160 Na^+//160K^+) and with 10 mM TEA^+ added to the internal solution. The membrane voltage was +60 mV; filtered at 4 kHz. (*B*) Single channel currents in control solution (160 Na^+//160 K^+) and with 1 mM TEA^+ added to the external solution. The membrane voltage was +120 mV; filtered at 4 kHz.

External TEA^+ is much more effective: a concentration of 1 mM reduces the channel currents by 75% even at +120 mV, and the voltage dependence of this block is also small [$\delta \approx 0.2$, $K_d(0) \approx 0.2$ mM]. If TEA^+ blocked at the same site regardless of which side it was applied to, the sum of the δ's for block from each side (that is, the sum of the fractional electrical distances) should be at least 1. In fact, the sum of the δ's measured is much smaller than 1, which indicates that TEA^+ blocks at different sites when applied to the outside or the inside. The different kinetics and affinities of the block are consistent with this (cf. Armstrong and Hille, 1972).

Comparison of C_9 Block Analyzed Directly and from Amplitude Histograms

Nonyltriethylammonium ion (C_9), a derivative of TEA with a long hydrocarbon chain attached, is known to block K^+ channels with high affinity (Armstrong, 1971; Armstrong and Hille, 1972; Vergara, 1983). When applied to the inside

---

FIGURE 3. (*opposite*) Blockade by Cs^+. (*A*) Single channel records in control solution (160 Na^+ outside, 160 K^+ inside; written 160 Na^+//160K^+) and with 10 mM Cs^+ added to the internal solution. The membrane voltage was +70 mV; filtered at 4 kHz. (*B*) Open channel *I-V* curves under the same condition as in *A*, measured from ramps. (*C*) The voltage dependence of internal and external Cs^+ block was measured as described in the text, according to Eq. 6. Internal Cs^+ block was treated by dividing the two ramps in *B*, point by point. The straight line was fitted to the data by a linear least-squares fit; it corresponds to values of $K_d(V = 0) = 85$ mM, $\delta = 0.18$. Points below 0 mV were not plotted, as they were significantly affected by noise in the *I-V* curves. External Cs^+ block was treated by dividing the two ramps in Fig. 2, *B* and *D*, treating the Na^+//K^+ *I-V* in Fig. 2*D* as the unblocked current i_0. The least-squares straight line corresponds to values of $K_d(0) = 160$ mM, $\delta = -0.95$.

face of Ca^{2+}-activated K^+ channels from T-tubule membrane, it produces a clearly resolvable block of current through the channels (Vergara, 1983), which is similar to the action of local anesthetics on endplate channels (Neher and Steinbach, 1978). C_9 is also an effective slow blocker of the Ca^{2+}-activated K^+

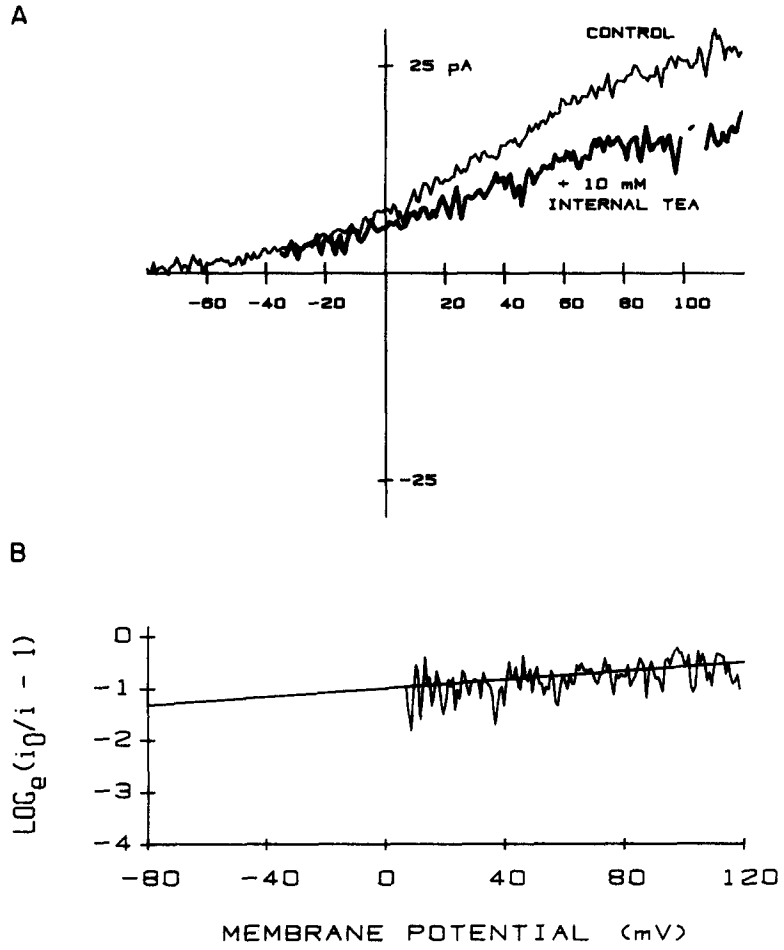

FIGURE 5. Voltage dependence of block by internal TEA^+. (*A*) Open channel *I-V* curves from ramps, under the same conditions as for Fig. 3*A*. (*B*) The data from panel *A* were treated as described for Fig. 3*C* to measure the voltage dependence of block. The straight line corresponds to values of $K_d = 24$ mM, $\delta = 0.1$.

channel in chromaffin cells. Fig. 6*A* shows the effect of 10 μM C_9 applied internally to a patch with Ca^{2+}-activated K^+ channels.

In order to test the validity and accuracy of the amplitude distribution method for determining block rates from records of flickery block, I studied blockade by this slow blocker, whose kinetics could be either measured directly from the

well-resolved records of blocking and unblocking, or analyzed by the amplitude distribution method.

The block and unblock rates of C_9 can be measured directly from the distributions of open and blocked durations during an opening burst. The open and closed time duration distributions, shown in Fig. 6, *B* and *C*, are reasonably well

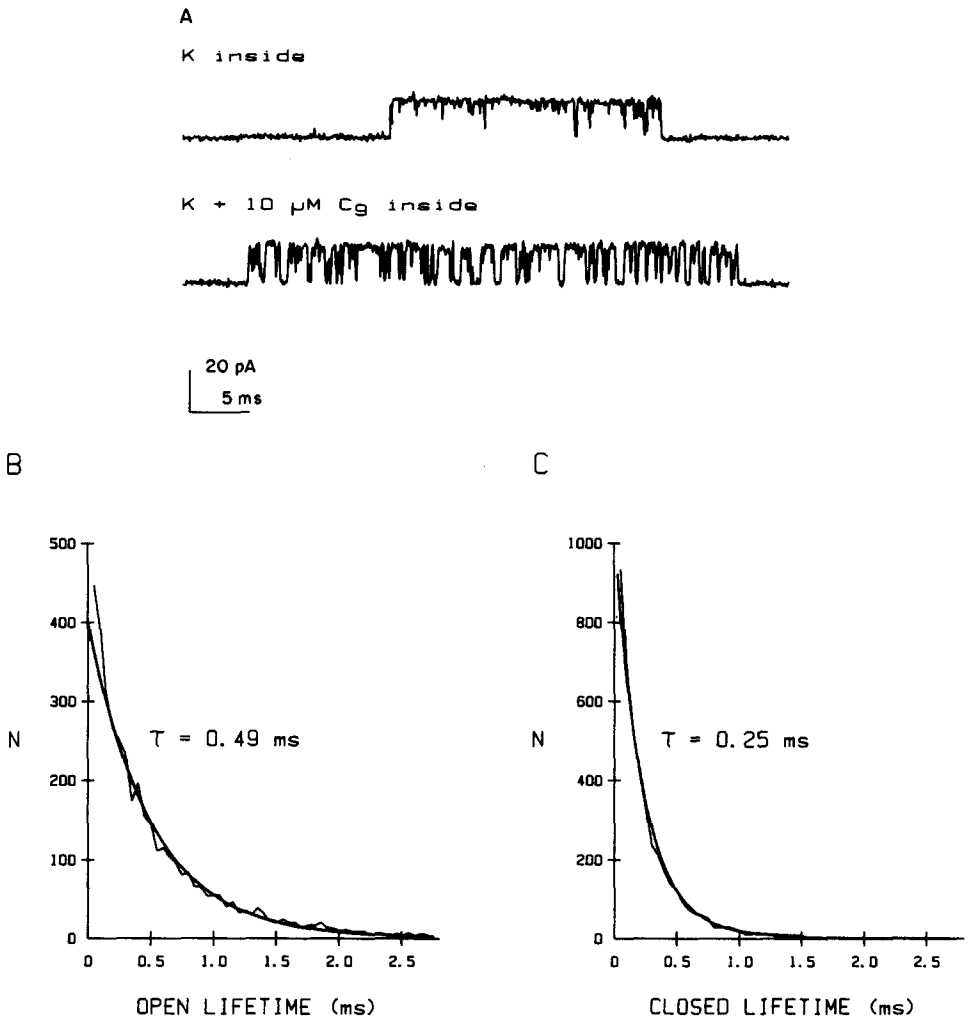

FIGURE 6. Block by internal C_9. (*A*) Single channel records in control solution (160 Na^+//160 K^+) and with 10 μM C_9 added to the internal solution. The membrane voltage was +60 mV; filtered at 8 kHz. (*B* and *C*) Open and closed lifetime duration distributions, with number of events (*N*) plotted against duration. The smooth lines were derived from straight lines fitted by eye to semilog plots of the data. The time constants are indicated. The closed lifetimes for normal channel closures were much longer than those due to C_9 block, and could be ignored on this time scale.

fitted by single exponentials; long closures and very brief flickers perturb the histograms very little, since the number of these events is small compared with the number of blocking events. The average blocked time measured by this method is 0.25 ms; the average open time (between block events) with 10 μM C_9 is 0.49 ms.

It is also possible, by heavily filtering the data with a filter slower than these block and unblock rates, to cause the blocking events to be ill resolved, and then

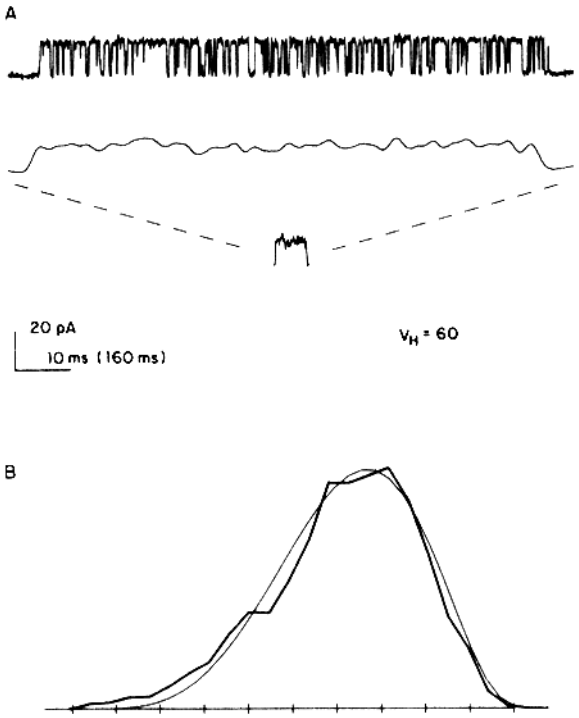

FIGURE 7. Re-analysis of C_9 block using the amplitude distribution method. (*A*) Refiltering of an 8-kHz record of internal C_9 block to simulate the poor resolution of the block produced by internal Na^+. Conditions as for Fig. 6*A*. The top trace is the original data; the middle trace was refiltered at 150 Hz; the bottom trace is the refiltered data on a 16-fold-compressed time scale. (*B*) Amplitude histogram (heavy line) of C_9 block records refiltered at 150 Hz. The smooth line was the best fit (by eye) to the data; it corresponds to values of τ_{open} = 0.47 ms, τ_{closed} = 0.27 ms.

to apply the amplitude distribution analysis to the same data. Data from channel currents with C_9 block were refiltered at 150 Hz to make the individual opening and closing events poorly resolved. As can be seen from a comparison of the 150-Hz refiltered data with the original 8-kHz data (Fig. 7*A*), each flicker corresponds to many blocking and unblocking events. An amplitude histogram was compiled from the refiltered data, and the parameters a and b were adjusted to give the best visual fit to the shape of the amplitude histogram (Fig. 7*B*).

Changes in *a* and *b* of ~2% give noticeable changes in the goodness of fit; in this case, where the open channel current in the absence of blocker is precisely known (from the unfiltered data, or from the control experiment without C_9), the ambiguity in fitting an individual empirical histogram is ~5% for each parameter. The open and blocked times determined by fitting the amplitude histogram are in excellent agreement with those determined by measuring the

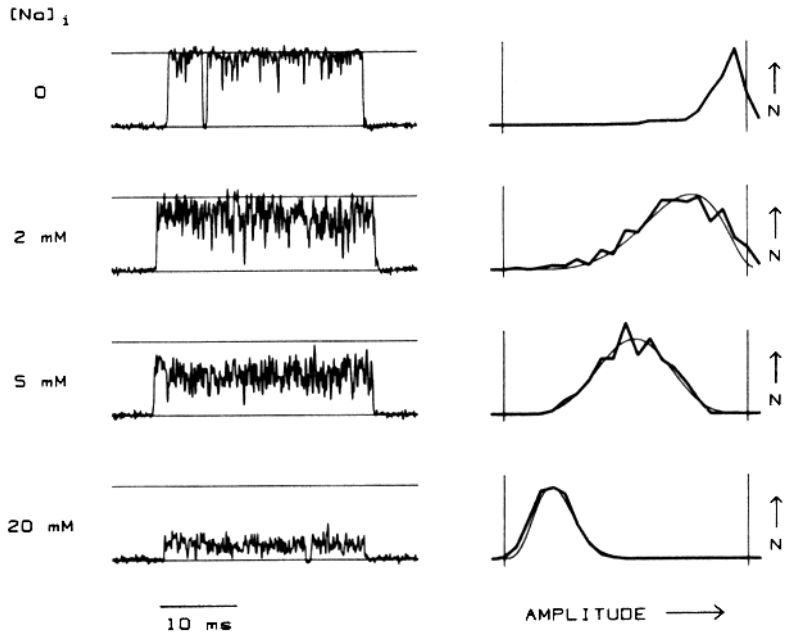

FIGURE 8. Flickery block by internal Na^+. (*Left*) Single channel records with the indicated concentration of Na^+ added to the internal solution containing 160 K^+ (the external solution contains 160 Na^+). The records are 40 ms long, and the lines indicate the baseline and open channel current (difference of 24.4 pA). The membrane voltage was +80 mV, and the data were filtered at 4 kHz. (*Right*) Amplitude histograms for each of the individual channel openings at left, plotted as number of occurrences (*N*) on the ordinate vs. amplitude on the abscissa. The left vertical line corresponds to the baseline amplitude and the right vertical line to the open channel amplitude (24.4 pA). Vertical scaling is arbitrary. The smooth curves superimposed on the lower three histograms are the theoretical beta distributions fitted empirically to the average histograms for many records.

durations directly. For the experiment shown, the average block time from the amplitude distribution fit was 0.27 ms, and the average open time was 0.47 ms.

Flickery Block by Internal Na^+

Millimolar quantities of Na^+ added to the medium bathing the intracellular face of a patch with Ca^{2+}-activated K^+ channels cause the open channel currents to diminish and to appear very noisy or flickery (Fig. 8; see also the report by

Marty, 1983).[1] The reduction in current increases with increasing Na concentration and is enhanced by positive membrane potentials, which suggests a voltage-dependent block of the channels by Na^+. Even at the practical recording limit of my patch clamp electronics (~10 kHz), the flicker induced by internal Na^+ cannot be resolved into discrete closings and openings that would correspond to blocking and unblocking events. The flicker can, however, be analyzed by the amplitude distribution method to determine the block and unblock rates.

Each amplitude histogram in the right half of Fig. 8 was compiled from the corresponding single channel opening event on the left. Many such bursts of channel activity were used to compile overall amplitude histograms for each

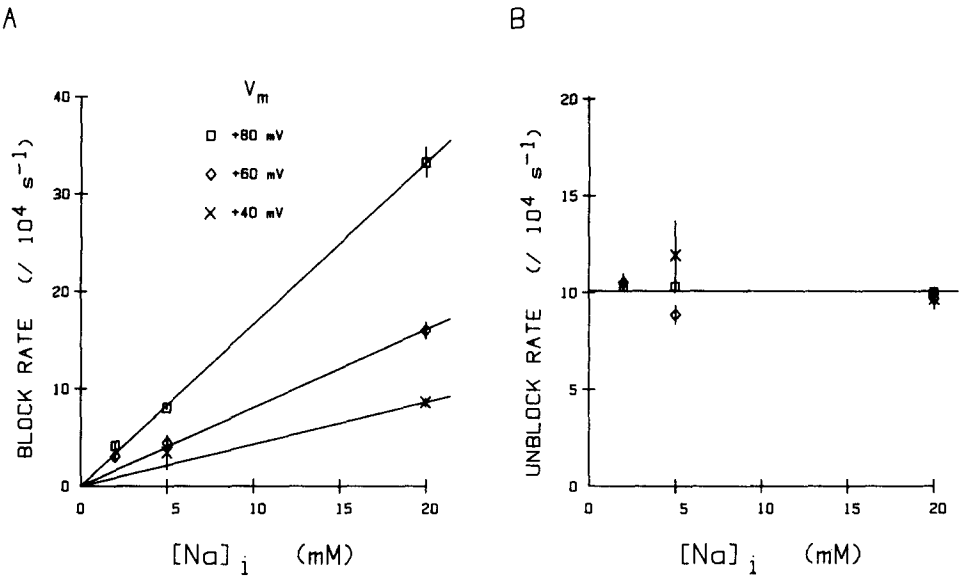

FIGURE 9. Block and unblock rates for internal Na^+ determined from amplitude distribution analysis. (*A*) Block rates (β). (*B*) Unblock rates (α). Each point is the mean ± SEM of between two and six separate histograms from experiments on four different patches. The external solution for all of these experiments contained 160 mM Na^+ and no K^+.

condition, and the block rate β and unblock rate α were adjusted to give the best fit of the theoretical distribution to the data. These theoretical fits are superimposed on the single-event amplitude histograms in Fig. 8. Fig. 9 shows the blocking and unblocking rates for Na^+ as determined from many such fits to amplitude histograms of channel flicker. The block rate increases linearly with Na^+ concentration, and the unblock rate is unaffected by Na^+ concentration. This is consistent with the hypothesis that Na^+ binding to the channel blocks

[1] All of these Na^+ block experiments were performed with an external solution that contained 160 mM NaCl and no K^+. External K^+ relieves block by Na^+, as described in the companion paper (Yellen, 1984*b*).

current flow, and that Na^+ dissociation from the channel allows current to pass again.

Block by internal Na^+ is very voltage dependent. The individual block and unblock rates measured by the amplitude distribution method show that the large voltage dependence of block resides almost entirely in the blocking rate. Fig. 10 shows the voltage dependence of the Na^+ entry rate (data pooled from 38 separate measurements on 4 patches at 3 different internal Na^+ concentrations). The block rate has a δ of 0.86, whereas the unblock rate has a δ indistinguishable from zero. This large and asymmetric voltage dependence proves to be critically important in deciding among models for permeation and blockade.

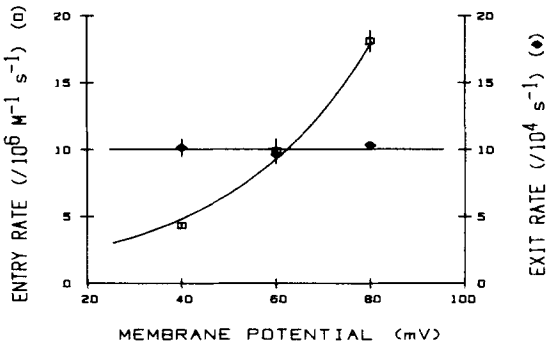

FIGURE 10. Voltage dependence of Na^+ entry and exit rates. The molar entry rate was determined by dividing the block rate (from Fig. 9) by the concentration of blocker (Na^+). The exponential curve is a best-fit exponential that rises e-fold per 29 mV; this corresponds to a value of $\delta = 0.86$. The horizontal line corresponds to $\delta = 0$. The points are mean ± SEM for pooled results from four patches, with n = 7, 13, and 18 for +40, +60, and +80 mV, respectively.

The Properties of Diffusion-limited Ion Flow Help Explain the Large Voltage Dependence of Na^+ Block

An Eyring rate theory model with two sites for ion binding and the possibility of multiple occupancy (Hodgkin and Keynes, 1955; Hladky, 1972; Läuger, 1973; see Hille and Schwarz, 1978, for a review) can easily explain all of the current-voltage data presented above for the Ca^{2+}-activated K^+ channel in chromaffin cell membranes. Similarly, the Woodhull (1973) model for block can explain the voltage dependence of Na^+ block. It is difficult, however, to explain both the permeation properties of the channel and the large voltage dependence of block in the context of a straightforward Eyring model for permeation (Yellen, 1984*a*). A common explanation for high voltage dependence of block in a multi-ion channel is that proposed by Hille and Schwarz: that a second ion enters the channel after the blocking ion and traps it (that is, slows its net exit rate). The voltage dependence of the entry of the second ion contributes to the net voltage dependence of block. This explanation cannot apply to the present case of Na^+ block, since the dominant voltage dependence of Na^+ block lies in the Na^+ entry step, not in the exit step.

A natural and likely explanation for the high voltage dependence of Na^+ block is diffusion limitation of ion flow through the channel. The rate of ion flux through high-conductance K^+ channels like those studied here is so large as to be comparable to the expected rate of ion diffusion up to the mouth of the channel (Hille, 1970; Hall, 1975; Latorre and Miller, 1983). Even the much smaller currents through the gramicidin A channel can be limited by diffusion under extreme conditions (Andersen and Procopio, 1980; Andersen, 1983*a–c*). Including such a diffusion limitation in the model for ion permeation through the Ca^{2+}-activated K^+ channel helps in two ways to explain the high voltage dependence of Na^+ entry into the channel.

First, diffusion limitation produces a decrease in channel occupancy at high voltages. When the K ion flow through a channel becomes comparable to the rate at which ions can diffuse up to the mouth, K^+ becomes depleted in the region near the mouth of the channel (the quantitative arguments for the effects discussed here were made by Läuger, 1976). The lowered concentration of K^+ near the mouth reduces its entry rate into the channel. This effect results in a lowered slope and eventually in saturation of the *I-V* curves at extreme voltages; hence sublinearity. The lowered entry rate also reduces the occupancy of the channel, increasing the opportunity for Na^+ to enter a vacant channel. Thus, the change in occupancy with voltage is one factor leading to an increased voltage dependence of Na^+ entry.

Second, diffusion limitation causes Na ions to be concentrated at the mouth of the channel at high voltages. Depletion of K^+ from the region near the mouth of the channel increases the resistance of the solution. Current flowing through the channel causes a voltage drop across this diffusional access resistance. This means, for positive voltages, that the voltage at the inner mouth of the channel will be more negative than the voltage of the internal solution. Thus, any cation, like Na^+, that is passively distributed (unlike K^+, which is depleted from this region by the high flux) will be concentrated at the mouth of the channel. This effect may be quite substantial. In order to achieve the high conductances observed for this channel, the intrinsic resistance of the channel must be nearly as low as the diffusional access resistance (Latorre and Miller, 1983), so the voltage drop across the diffusional access resistance may be a significant percentage of the total. If 30% of the transmembrane voltage were to drop across the diffusional access resistance on the intracellular side, then Na^+ entry into the channel would have an effective valence of 0.3, even in the absence of any other contributions to the voltage dependence of Na^+ entry.

Both sources of voltage dependence affect only the entry rate and not the exit rate. The perturbation in ion concentrations that produces the effects disappears very quickly when ion flow stops, as when a Na ion enters and blocks the channels. This relaxation probably takes on the order of 10^{-11} s (Läuger, 1976), as compared with a residence time for the Na ion on the order of 10^{-6} s.

A Model That Fits the I-V and Voltage Dependence Data

In order to show that the properties of diffusion-limited ion flow can explain the voltage dependence of Na^+ entry, a numerical model was constructed that

combines diffusion limitation with a two-site Eyring rate theory model for permeation. The details of the model are shown here only to demonstrate its adequacy, and they should not be understood as a detailed description of the channel.

This model incorporates features of the model for ion permeation through gramicidin A (Hladky, 1972; Eisenman et al., 1978; for a review, see Finkelstein and Andersen, 1981) and features of the single-file, multi-ion model for delayed rectifier K^+ channels (Hodgkin and Keynes, 1955; Armstrong, 1975*a*, *b*; Hille and Schwarz, 1978). The essential features of the model are the presence of two sites for ion binding that may both be occupied simultaneously, repulsion between ions occupying the two sites, and diffusion limitation of ion flow.

Läuger (1976) solved the radially symmetric electrodiffusion problem of a hemispherical channel mouth, with boundary conditions for the voltage and ion concentrations far from the channel mouth ($r = \infty$). Outside of this hemisphere, free electrodiffusion obtains; inside this hemisphere, the channel has the usual restricted diffusion (jump) properties of an Eyring permeation model (Eyring et al., 1949) with saturable sites and multiple occupancy.

An iterative procedure was used to solve simultaneously the electrodiffusion equations for diffusion-limited ion flow and the rate equations for the two-site Eyring model. Fig. 11 shows the model scheme and the numbers used in modeling; these numbers should not be taken at all literally, since they depend on the (unknown) absolute frequency factors in Eyring rate theory, and since many possible combinations of values give a reasonable fit to the experimental data. Cs^+ and Na^+ were treated as impermeant species; Rb^+ was treated as a permeant species distinct from K^+. The effective capture radii postulated in the model are 0.2 and 0.14 nm for the outside and inside mouths of the channel, respectively (the capture radius is roughly the difference between the radius of the hemisphere and the radius of the diffusing ion; Läuger, 1976; Andersen, 1983*a*). These values are comparable to that hypothesized for the gramicidin A channel (0.05 nm) on the basis of both physical and electrophysiological data (see Andersen and Procopio, 1980). The energy barriers to K^+ entry are very small, which keeps the intrinsic resistance of the channel low and comparable to the diffusion resistance. The small barriers only slightly perturb the rate of entry of ions to the channel, which is essentially limited by electrodiffusion.

The model gives current-voltage relationships for the channel under biionic conditions; these are shown superimposed upon the experimental *I-V*'s in Fig. 2. The energies for the outer barrier and site were constrained to be the same for K^+, Cs^+, and Rb^+, because of the identical efficacy of these three ions in relieving Na^+ block (see Yellen, 1984*b*). After fitting the *I-V* in symmetrical K^+, the *I-V* with Na^+ outside was well fitted simply by assuming that Na^+ acts as an inert, impermeant substitute for K^+ outside.

Multiple occupancy and repulsion between ions in the channel are included in the model to explain the "knock-off" effect that external K, Rb, or Cs ions have on block by internal Na^+ (Yellen, 1984*b*). When a 10-mM concentration of one of these ion species is present in the external bathing medium, the rate of Na^+ exit in the model is increased 2.9-fold, which is comparable to the experimental value of ~3.

The voltage dependence for Na^+ entry near +60 was computed, taking into account three contributing factors: the intrinsic barrier structure, the concentration of Na^+ in the convergence region, and the change in channel occupancy. The voltage dependence conferred by the intrinsic barrier structure was reduced by the effect of diffusion limitation: in the model used, 40% of the transchannel field fell across the entry barrier, but this was only 22% of the total transmembrane field, since some of the voltage drop fell across the convergence regions. The voltage drop of ~35% of the field across the inner convergence region raised the Na^+ concentration over that in the bulk solution by a factor of $\exp(0.35 \times FV/RT)$, causing an additive increase of 0.35 in δ. The availability of the inner site of the channel increased by 10% on raising the voltage from 50 to 60 mV; this corresponds to an effective increase in δ of 0.22. The total voltage dependence of Na^+ entry in the model has a value of $\delta = 0.79$, which is close to the experimental value of 0.86. Thus, including diffusion limitation in the permeation model helps explain the high voltage dependence of Na^+ entry together with the permeation properties of other ions in the channel.

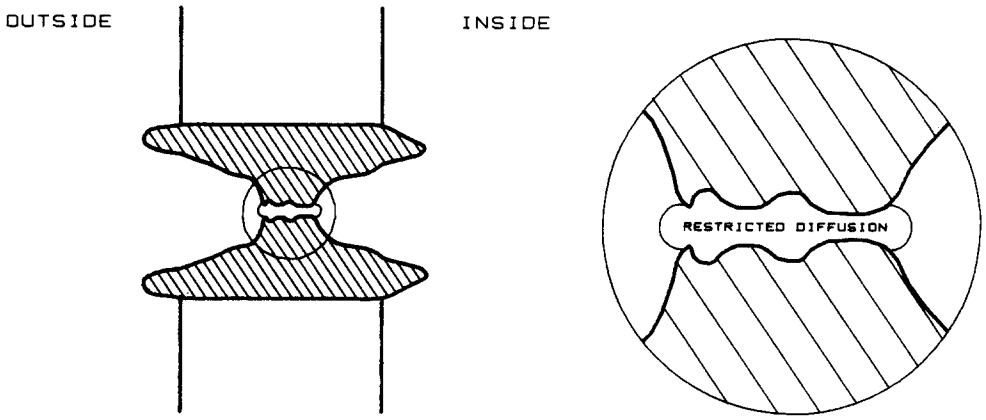

ION	B1	W1	W2	B2
K	0.5	-7.2	-9.0	0.6
Cs	0.5	-7.2	-9.0	***
Rb	0.5	-7.2	-10.2	1.2
Na	***	***	-9.0	5.2

BARRIER AND WELL ENERGIES

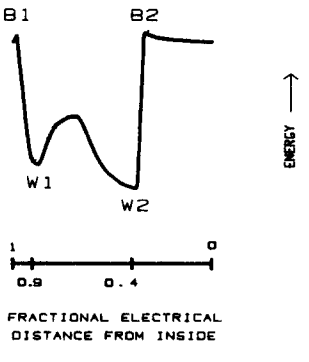

DISCUSSION

Channel Selectivity

The selectivity of this chromaffin cell Ca^{2+}-activated K^+ channel is not unusual among K^+ channels. Only a few ions have been studied in the present work, and they follow a familiar pattern: K^+ passes through the channel much better than does Na^+, Cs^+ blocks the channel, and Rb^+ is nearly as permeable as K^+ but also blocks the channel. The behavior of these ions in this channel is similar to their behavior in the delayed rectifier of squid (Chandler and Meves, 1965; Adelman and Senft, 1966; Bezanilla and Armstrong, 1972) and node of Ranvier (Bergman, 1970; Hille, 1973), though different from that in snail neuron, which is not blocked by Rb^+, and which passes Cs^+ current (Reuter and Stevens, 1980). This channel is more selective than the large-conductance K^+ channel in sarcoplasmic reticulum, which has a significant permeability to Na^+ (Coronado et al., 1980). The permeability properties of a very similar Ca^{2+}-activated K^+ channel from skeletal muscle T-tubule membranes has been studied by Vergara (1983); re-

FIGURE 11. (*opposite*) Features of a permeation model for the Ca^{2+}-activated K^+ channel. At the upper left is a cartoon of the channel showing the wide vestibules; by the reasoning of Latorre and Miller (1983), the region of restricted diffusion for this channel should traverse only a fraction of the transmembrane distance. At the upper right is an expanded diagram of the small part of the channel; between the two hemispherical boundaries at the mouths, restricted diffusion (Eyring-model) obtains. The two broader regions in the channel indicate the location in the model of the two binding sites (they do not denote a swelling of the channel diameter). Beneath this diagram (lower right) is the energy diagram for a K ion traversing the channel, with labels for the two barrier energy peaks (B1, B2) and the two energy wells (W1, W2). The fractional electrical distance from the inside solution (in the absence of ion flow) is indicated on the ruler; electrical distance need not be congruent with physical distance. When current flows, part of the total voltage drop falls between the bath solution and the hemispherical boundary at the mouth of the channel (i.e., across the diffusional access resistance). The model is an Eyring rate theory model, like that of Hille and Schwarz (1978), with two sites for ion binding. The sites are at equilibrium with one another; the jump rate to the outside is relatively slow. Diffusion limitation has been added to the model, as described in the text; the capture radii chosen for the fit are 2 and 1.4 Å for the outside and inside mouths of the channel, respectively. The repulsion between ions is expressed by two factors: the entry rate of an ion to one site is reduced by a factor of 5 when the other site is occupied (f_{in} = 1/5), and the exit rate of an ion is increased by a factor of 40 when the other site is occupied (f_{out} = 40). The pre-exponential (frequency factors, ν_{in} and ν_{out}, used in the model are both equal to 10^{11}. The barrier and well energies for each ion are given in the lower left part of the figure. Energy values are in units of kT (approximately equal to 0.6 kcal/mol). Asterisks (***) mean that the indicated part of the channel is inaccessible to each ion. The very small barriers to ion entry are too small to satisfy the assumptions of absolute rate theory; they must be understood only as small perturbations to the entry rate, which is determined by diffusion limitation.

markably, the T-tubule channel does not pass Rb^+ ($P_{Rb}/P_K < 0.1$, as defined by the reversal potential; current does not reverse below +60 mV with K^+ outside, Rb^+ inside), whereas the chromaffin cell channel is quite permeable to Rb^+ ($P_{Rb}/P_K \approx 0.83$ from the reversal potential of −5 mV with Rb^+ outside and K^+ inside).

Open Channel Flicker

The present paper shows that one cause of flicker in single channel currents can be ionic blockade. Internal Na^+ increases the flicker in single open channel currents through Ca^{2+}-activated K^+ channels, in a fashion consistent with voltage-dependent blockade by Na^+.

This flicker can be analyzed by analyzing its amplitude distribution. The analysis depends on two assumptions: first, that the flicker is composed of filtered fluctuations between two discrete conductance states of known conductance, and second, that the transitions between the two states are described by a simple two-state Poisson process. In the present case of Na^+ block, the first assumption seems reasonable. In the absence of Na^+, the conductance of the open channel can be determined; in the presence of excess Na^+, current through the completely blocked channel is zero. It seems reasonable to think that at intermediate Na^+ concentrations, the channel fluctuates between the completely blocked and completely open states. The second assumption seems to be correct in cases where the blocking events can be well resolved in time, like the C_9 block described in the present paper and the local anesthetic block of endplate channels (Neher and Steinbach, 1978). The excellent fits between the predicted amplitude distributions and the measured distributions support the assumption in the present case, as do the reasonable results of the analysis, which show that the rate of entering the blocked state depends linearly on $[Na^+]$ and that the rate of reopening is independent of $[Na^+]$.

The method of amplitude distribution analysis can be applied to any process that satisfies the assumptions and has transition rates slower than ~20 times the settling rate of the recording system. The latter is a practical limitation; processes faster than this are so poorly resolved that the analysis will depend critically on background noise. Noise from the instrumentation and from the open channel (see below) always tends to broaden the amplitude distribution; this makes only a small fractional change in the broad distributions produced by slow processes, but a significant change in the narrow distributions produced by fast processes. Processes slower than twice the settling rate must be refiltered with a slower filter if they are to be analyzed by this method, since the fits of the amplitude distributions of very slow processes are also very uncritical. It is also difficult to analyze processes whose forward and backward rates are very different (more than about fivefold); this is no problem in studying block processes, whose forward rates can be manipulated by changing the blocker concentration.

The conductance of the two states that contribute to the flicker must be known. In the present case, we can be confident that the conductance of the blocked channel is negligible, since high Na^+ concentrations drive the current amplitude to the zero-current level.

Other Sources of Flicker and Noise in Open Channel Currents

Processes other than block can produce brief closings or flickers. Conformational changes have been proposed to explain flicker in the Ca^{2+}-activated K^+ channel (Magleby and Pallotta [1983] in myotubes; Moczydlowski and Latorre [1983] in reconstituted channels from rat muscle) and in the acetylcholine (ACh)-activated channel (Colquhoun and Sakmann, 1981; Dionne and Leibowitz, 1982).

Opening and closing processes that are much slower or much more infrequent than the flicker produced by block do not significantly interfere with the amplitude distribution analysis. No attempt is made to avoid including brief closings (of ~1–5 ms) in compiling the amplitude histograms. There cannot be more than ~100 of these events included in the typical histogram, which contains ~10,000 blocking events (based on the total time and the rates of the block process). These closures contribute only to the baseline peak of the amplitude histogram, which is separated and subtracted before analyzing the histogram to determine block rates.

Excess noise in the open channel currents (above the noise present when the channel is closed) has been studied by Sigworth (1982). He attributes the high-frequency component of this open channel noise in the ACh-activated channel of myotubes to rapid block by H ions. This corresponds to a very fast flicker process. There is, in addition, a low-frequency component to the noise that may reflect small fluctuations in the open channel conductance, perhaps because of channel breathing.

Processes such as these that increase the noise of the open channel will tend to broaden the amplitude distributions and produce errors in the values derived from amplitude distribution analysis. There is no evidence for any significant excess open channel noise for currents through the Ca^{2+}-activated channel.

Diffusion-limited Ion Flow

The work presented here contains no direct evidence for the importance of diffusion limitation of ion flow through the Ca^{2+}-activated K^+ channel. Diffusion limitation nevertheless seems likely to be important for this channel. Latorre and Miller (1983) have directly discussed the apparent paradox of such a large-conductance channel that is also very selective; they show that this combination is not merely counter-intuitive but actually quantitatively difficult to explain. The difficulty is that the high rate of flux through a channel like this Ca^{2+}-activated K^+ channel is comparable to the rate of diffusion up to a small aperture. Thus, it takes special effort to design a model for a channel that carries as much current as this one does, and that model is likely to show diffusion-limited ion flow.

The ease of explaining the voltage dependence of Na^+ block when diffusion limitation is added to an Eyring model also makes diffusion limitation an appealing hypothesis for this channel. Diffusion limitation has been shown to be important for the gramicidin A channel. Andersen and Procopio (1980) showed that the current through the gramicidin A channel saturates at high voltages, with permeant ion concentrations of <1 M. This limiting current can be reduced

by raising the viscosity of the bathing solution with sucrose, which has the effect of slowing ion diffusion through the solution. This decrease, as well as the magnitude of the limiting current, is consistent with the predictions for diffusion-limited ion flow (Läuger, 1976). Andersen (1983*a–c*) has provided further support for the importance of diffusion limitation for the gramicidin A channel. It should be possible by a similar series of experiments to test directly the hypothesis that diffusion limitation is also important for the Ca^{2+}-activated K^+ channel.

APPENDIX

Amplitude Distribution with a First-Order Filter

FitzHugh (1983) has treated this problem generally and in detail. I present here a less general and less rigorous but simpler derivation, which is suggested by the treatment of diffusion in one dimension.

The filtered, two-state process is composed of a deterministic process (the filter relaxation) and a stochastic process (blocking and unblocking). For a first-order filter, the time derivative of the filter output y is described by

$$\dot{y} = -(y - c)/\tau, \tag{A1}$$

where c is the value at the filter input and τ is the time constant of the filter.

The first step in combining the filtering process with the blocking-unblocking process is to describe the amplitude of the output of the filter in probabilistic terms. Let us consider an ensemble of 1,000 identical filters (systems) with time constant τ and a random distribution of starting values (y). The starting values can be described by a probability density function:

$f(y)\,dy$ = probability of a starting value in the interval $(y, y + dy)$
= (number of filters with outputs between y and $y + dy$)/1,000.

At time 0, we drive the input of all of the filters to zero. We can describe the evolution of the filter outputs in the next instant dt by using the differential Eq. A1 with $c = 0$ to find that $\dot{y} = -y/\tau$. This means that a filter whose output was exactly y at time 0 will have an output of $y - \delta(y)$ at time dt, where

$$\delta(y) = y/\tau\ dt. \tag{A2}$$

Thus, filters that started with outputs between $y + \delta(y)$ and $y + dy + \delta(y + dy)$ will decay into the interval $(y, y + dy)$; those that started in the interval $[y, y + \delta(y)]$ will decay below y. The net change in $f(y)$ will be the former minus the latter, or

$$df(y)\,dy = f(y + dy)\delta(y + dy) - f(y)\delta(y). \tag{A3}$$

Dividing both sides by dt and dy gives an expression for the time derivative of the density function:

$$df(y)/dt = d/dy\ [f(y)\ y/\tau]. \tag{A4}$$

This is analogous to a modified one-dimensional diffusion process, where $f(y)$ is a concentration and y/τ is the rate of flux at y.

We can now include the blocking-unblocking process. Let the transition rate from blocked to open be α, and from open to blocked, β. The probability of a channel being

open, p_o, is $\alpha/(\alpha + \beta)$; the probability of a channel being blocked is $p_b = \beta/(\alpha + \beta)$. In a small period of time dt, the probability that a blocked channel will become unblocked is αdt, and similarly the probability that an open channel will become blocked is βdt. Now let us take 1,000 channels, measure their current with 1,000 patch clamps, and pass the output through our 1,000 filters.

When a channel is blocked, the filter output relaxes toward zero (and eventually reaches a constant value of zero); when a channel is open, the filter output relaxes toward one. Thus, we will define two separate conditional probability density functions $f_b(y)$ and $f_o(y)$ to describe the filter behavior when the channel is blocked or open, respectively. The joint probability that a channel is open and that the filter output lies in $(y, y + dy)$ is given by $p_o f_o(y)dy$, so the number of systems fitting this description is $1{,}000 p_o f_o(y)dy$. When one of these open channels becomes blocked, this number will decrease by one, and the corresponding number of blocked channels $1{,}000 p_b f_b(y)dy$ will increase by one. We can finally write a pair of differential equations describing the filtered process:

$$d/dt\,[p_b f_b(y)] = d/dy\,[p_b f_b(y)\, y/\tau] - \alpha p_b f_b(y) + \beta p_o f_o(y); \tag{A5a}$$

$$d/dt\,[p_o f_o(y)] = d/dy\,[p_o f_o(y)\,(y - 1)/\tau] - \beta p_o f_o(y) + \alpha p_b f_b(y). \tag{A5b}$$

In each equation, the first term corresponds to the filter relaxation process, the second term to the channels leaving the indicated state, and the third to the channels entering from the other state. These equations can be solved in the steady state (with the left-hand sides set to zero) to yield an overall probability density for the amplitude of the filter output:

$$f(y) = p_o f_o(y) + p_b f_b(y) \tag{A6}$$

$$= y^{a-1}(1 - y)^{b-1}/B(a, b), \tag{A7}$$

where

$$a = \alpha\tau, \qquad b = \beta\tau, \tag{A8a, b}$$

and

$$B(a, b) = \int_0^1 y^{a-1}(1 - y)^{b-1}dy \qquad \text{(beta function)}. \tag{A9}$$

This distribution, defined for y on the interval (0, 1), is called a beta distribution; the beta function serves to normalize it. It describes the amplitude distribution of a two-state process with rates α and β after filtering with a first-order filter of time constant τ.

I thank Rick Aldrich, David Corey, and Chuck Stevens for helpful discussions and for their remarks on the manuscript. I also thank Clay Armstrong, Knox Chandler, and Dick Tsien for critically reading an earlier version.

This work was supported by grant NS 12961 to C. F. Stevens and by Training Grant GM 7527 from the National Institutes of Health. Gary Yellen is a Hoffmann-La Roche Fellow of the Life Sciences Research Foundation.

Received for publication 30 January 1984 and in revised form 20 April 1984.

REFERENCES

Adams, D. J., W. Nonner, T. M. Dwyer, and B. Hille. 1981. Block of endplate channels by permeant cations in frog skeletal muscle. *J. Gen. Physiol.* 78:593–615.

Adelman, W. J., Jr., and R. J. French. 1978. Blocking of the squid axon potassium channel by external caesium ions. *J. Physiol. (Lond.).* 276:13–25.

Adelman, W. J., Jr., and J. P. Senft. 1966. Voltage clamp studies on the effect of internal cesium ion on sodium and potassium currents in the squid giant axon. *J. Gen. Physiol.* 50:279–293.

Andersen, O. S. 1983*a*. Ion movement through gramicidin A channels: single-channel measurements at very high potentials. *Biophys. J.* 41:119–133.

Andersen, O. S. 1983*b*. Ion movement through gramicidin A channels: interfacial polarization effects on single-channel current measurements. *Biophys. J.* 41:135–146.

Andersen, O. S. 1983*c*. Ion movement through gramicidin A channels: studies on the diffusion-controlled association step. *Biophys. J.* 41:147–165.

Andersen, O. S., and J. Procopio. 1980. Ion movement through gramicidin A channels: on the importance of the aqueous diffusion resistance and ion-water interactions. *Acta Physiol. Scand. Suppl.* 481:27–35.

Armstrong, C. M. 1966. Time course of TEA^+-induced anomalous rectification in squid giant axons. *J. Gen. Physiol.* 50:491–503.

Armstrong, C. M. 1971. Interaction of tetraethylammonium ion derivatives with the potassium channels of giant axons. *J. Gen. Physiol.* 58:413–437.

Armstrong, C. M. 1975*a*. Potassium pores of nerve and muscle membranes. *In* Membranes: A Series of Advances. G. Eisenman, editor. Marcel Dekker, New York. 3:325–358.

Armstrong, C. M. 1975*b*. Ionic pores, gates and gating currents. *Q. Rev. Biophys.* 7:179–210.

Armstrong, C. M., and L. Binstock. 1965. Anomalous rectification in the squid giant axon injected with tetraethylammonium chloride. *J. Gen. Physiol.* 48:859–872.

Armstrong, C. M., and B. Hille. 1972. The inner quaternary ammonium ion receptor in potassium channels of the node of Ranvier. *J. Gen. Physiol.* 59:388–400.

Bergman, C. 1970. Increase of sodium concentration near the inner surface of the nodal membrane. *Pflügers Arch. Eur. J. Physiol.* 317:287–302.

Bezanilla, F., and C. M. Armstrong. 1972. Negative conductance caused by entry of sodium and cesium ions into the potassium channels of squid axons. *J. Gen. Physiol.* 60:588–608.

Chandler, W. K., and H. Meves. 1965. Voltage clamp experiments on internally perfused giant axons. *J. Physiol. (Lond.).* 180:788–820.

Colquhoun, D., and B. Sakmann. 1981. Fluctuations in the microsecond time range of the current through single acetylcholine receptor ion channels. *Nature (Lond.).* 294:464–466.

Colquhoun, D., and F. J. Sigworth. 1983. Fitting and statistical analysis of single-channel records. *In* Single-Channel Recording. B. Sakmann and E. Neher, editors. Plenum Publishing, New York. 191–263.

Cook, D. L., M. Ikeuchi, and W. J. Fujimoto. 1983. Patch-clamp study of calcium-activated potassium conductance in pancreatic islet cells. *Soc. Neurosci. Abstr.* 9(1):22.

Coronado, R., and C. Miller. 1979. Voltage-dependent caesium blockade of a cation channel from fragmented sarcoplasmic reticulum. *Nature (Lond.).* 280:807–810.

Coronado, R., R. Rosenberg, and C. Miller. 1980. Ionic selectivity, saturation, and block in a K^+-selective channel from sarcoplasmic reticulum. *J. Gen. Physiol.* 76:425–446.

Dionne, V. E., and M. D. Leibowitz. 1982. Acetylcholine receptor kinetics: a description from single-channel currents at snake neuromuscular junctions. *Biophys. J.* 39:253–261.

Dubois, J. M., and C. Bergman. 1977. The steady-state potassium conductance of the Ranvier node at various external K-concentrations. *Pflügers Arch. Eur. J. Physiol.* 370:185–194.

Eisenman, G., J. P. Sandblom, and E. Neher. 1978. Interactions in cation permeation through

the gramicidin channel: Cs, Rb, K, Na, Li, Tl, H, and effects of anion binding. *Biophys. J.* 22:307–340.

Eyring, H., R. Lumry, and J. W. Woodbury. 1949. Some applications of modern rate theory to physiological systems. *Rec. Chem. Prog.* 10:100–114.

Finkelstein, A., and O. S. Andersen. 1981. The gramicidin A channel: a review of its permeability characteristics with special reference to the single-file aspect of transport. *J. Membr. Biol.* 59:155–171.

FitzHugh, R. 1983. Statistical properties of the asymmetric random telegraph signal, with applications to single-channel analysis. *Math. Biosci.* 64:75–89.

Gorman, A. L. F., J. C. Woolum, and M. C. Cornwall. 1982. Selectivity of the Ca^{2+}-activated and light-dependent K^+ channels for monovalent cations. *Biophys. J.* 38:319–322.

Hagiwara, S., and K. Takahashi. 1974. The anomalous rectification and cation selectivity of the membrane of a starfish egg cell. *J. Membr. Biol.* 18:61–80.

Hall, J. E. 1975. Access resistance of a small circular pore. *J. Gen. Physiol.* 66:531–532.

Hamill, O. P., A. Marty, E. Neher, B. Sakmann, and F. J. Sigworth. 1981. Improved patch-clamp techniques for high-resolution current recording from cells and cell-free membrane patches. *Pflügers Arch. Eur. J. Physiol.* 391:85–100.

Hermann, A., and A. L. F. Gorman. 1981. Effects of tetraethylammonium on potassium channels in a molluscan neuron. *J. Gen. Physiol.* 78:87–110.

Hille, B. 1967. The selective inhibition of delayed potassium currents in nerve by tetraethylammonium ion. *J. Gen. Physiol.* 50:1287–1302.

Hille, B. 1970. Ionic channels in nerve membranes. *Prog. Biophys. Mol. Biol.* 21:3–32.

Hille, B. 1972. The permeability of the sodium channel to metal cations in myelinated nerve. *J. Gen. Physiol.* 59:637–658.

Hille, B. 1973. Potassium channels in myelinated nerve: selective permeability to small cations. *J. Gen. Physiol.* 61:669–686.

Hille, B. 1975. Ionic selectivity of Na and K channels of nerve membranes. *In* Membranes: A Series of Advances. G. Eisenman, editor. Marcel Dekker, New York. 3:255–323.

Hille, B., and W. Schwarz. 1978. Potassium channels as multi-ion single-file pores. *J. Gen. Physiol.* 72:409–442.

Hladky, S. B. 1972. The mechanism of ion conduction in thin lipid membranes containing gramicidin A. Ph.D. Thesis. Cambridge University, Cambridge, England.

Hodgkin, A. L., and R. D. Keynes. 1955. The potassium permeability of a giant nerve fibre. *J. Physiol. (Lond.).* 128:61–88.

Horn, R., and J. Patlak. 1980. Single channel currents from excised patches of muscle membrane. *Proc. Natl. Acad. Sci. USA.* 77:6930–6934.

Horn, R., J. Patlak, and C. F. Stevens. 1981. The effect of tetramethylammonium on single sodium channel currents. *Biophys. J.* 36:321–327.

Kilpatrick, D. L., F. H. Ledbetter, K. A. Carson, A. G. Kirshner, R. Slepetis, and N. Krishner. 1980. Stability of bovine adrenal medulla cells in culture. *J. Neurochem.* 35:679–692.

Latorre, R., and C. Miller. 1983. Conduction and selectivity in potassium channels. *J. Membr. Biol.* 71:11–30.

Läuger, P. 1973. Ion transport through pores: a rate-theory analysis. *Biochim. Biophys. Acta.* 311:423–441.

Läuger, P. 1976. Diffusion-limited ion flow through pores. *Biochim. Biophys. Acta.* 455:493–509.

Magleby, K. L., and B. S. Pallotta. 1983. Calcium dependence of open and shut interval

distributions from calcium-activated potassium channels in cultured muscle. *J. Physiol. (Lond.).* 344:585–604.

Martell, A. E., and R. M. Smith. 1974. Critical Stability Constants. Plenum, London. 1:269.

Marty, A. 1981. Ca-dependent K channels with large unitary conductance in chromaffin cell membranes. *Nature (Lond.).* 291:497–500.

Marty, A. 1983. Blocking of large unitary calcium-dependent potassium currents by internal sodium ions. *Pflügers Arch. Eur. J. Physiol.* 396:179–181.

Methfessel, C., and G. Boheim. 1982. The gating of single calcium-dependent potassium channels is described by an activation/blockade mechanism. *Biophys. Struct. Mech.* 9:35–60.

Moczydlowski, E., and R. Latorre. 1983. Gating kinetics of Ca^{2+}-activated K^+ channels from rat muscle incorporated into planar lipid bilayers. Evidence for two voltage-dependent Ca^{2+} binding reactions. *J. Gen. Physiol.* 82:511–542.

Neher, E., and J. H. Steinbach. 1978. Local anaesthetics transiently block currents through single acetylcholine-receptor channels. *J. Physiol. (Lond.).* 277:153–176.

Reuter, H., and C. F. Stevens. 1980. Ion conductance and ion selectivity of potassium channels in snail neurones. *J. Membr. Biol.* 57:103–118.

Sigworth, F. J. 1982. Fluctuations in the current through open ACh-receptor channels. *Biophys. J.* 37:309*a*. (Abstr.)

Tasaki, I., and S. Hagiwara. 1957. Demonstration of two stable potential states in the squid giant axon under tetraethylammonium chloride. *J. Gen. Physiol.* 40:859–885.

Thompson, S. H. 1977. Three pharmacologically distinct potassium channels in molluscan neurones. *J. Physiol. (Lond.).* 265:465–488.

Vergara, C. 1983. Characterization of a Ca^{2+}-activated K^+ channel from skeletal muscle membranes in artificial bilayers. Ph.D. Dissertation. Harvard University, Cambridge, MA.

Wilson, S. P., and H. Viveros. 1981. Primary culture of adrenal medullary chromaffin cells in a chemically defined medium. *Exp. Cell Res.* 133:159–169.

Wong, B. S., H. Lecar, and M. Adler. 1982. Single calcium-dependent potassium channels in clonal anterior pituitary cells. *Biophys. J.* 39:313–317.

Woodhull, A. M. 1973. Ionic blockage of sodium channels in nerve. *J. Gen. Physiol.* 61:687–708.

Yellen, G. 1982. Single Ca^{2+}-activated nonselective cation channels in neuroblastoma. *Nature (Lond.).* 296:357–359.

Yellen, G. 1984*a*. Ionic permeation and blockade in calcium-activated potassium channels of chromaffin cells. Ph.D. Dissertation. Yale University, New Haven, CT.

Yellen, G. 1984*b*. Relief of Na^+ block of Ca^{2+}-activated K^+ channels by external cations. *J. Gen. Physiol.* 84:187–199.